AD-A144 245 TEMPERATURE COMPENSATION OF SURFACE TRANSVERSE WAVES FOR STABLE OSCILLATO..(U) STANFORD UNIV CALIF W W HANSEN LABS OF PHYSICS B A AULD JUN 84 RADC-TR-84-142 1/1

UNCLASSIFIED F19628-83-K-0011 F/G 20/14 NL

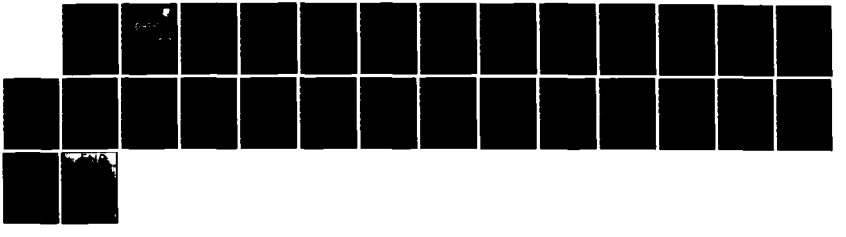

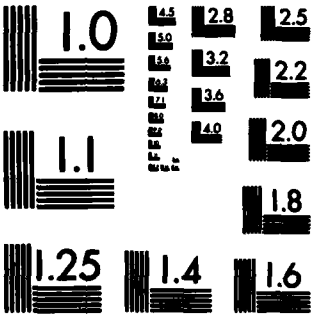


MICROCOPY RESOLUTION TEST CHART
NATIONAL BUREAU OF STANDARDS-1963-A

(12)

RADC-TR-84-142
Interim Report
June 1984

# TEMPERATURE COMPENSATION OF SURFACE TRANSVERSE WAVES FOR STABLE OSCILLATOR APPLICATIONS

Stanford University

B. A. Auld



APPROVED FOR PUBLIC RELEASE; DISTRIBUTION UNLIMITED

ROME AIR DEVELOPMENT CENTER
Air Force Systems Command
Griffiss Air Force Base, NY 13441

This report has been reviewed by the RADC Public Affairs Office (PA) and is releasable to the National Technical Information Service (NTIS). At NTIS it will be releasable to the general public, including foreign nations.

RADC-TR-84-142 has been reviewed and is approved for publication.

APPROVED: Paul H. Carr

PAUL H. CARR
Project Engineer

APPROVED: Allan C. Schell

ALLAN C. SCHELL
Chief, Electromagnetic Sciences Division

FOR THE COMMANDER: John A. Ritz

JOHN A. RITZ
Acting Chief, Plans Office

If your address has changed or if you wish to be removed from the RADC mailing list, or if the addressee is no longer employed by your organization, please notify RADC (EEA) Hanscom AFB MA 01731. This will assist us in maintaining a current mailing list.

Do not return copies of this report unless contractual obligations or notices on a specific document requires that it be returned.

UNCLASSIFIED
SECURITY CLASSIFICATION OF THIS PAGE

## REPORT DOCUMENTATION PAGE

| | |
|---|---|
| 1a. REPORT SECURITY CLASSIFICATION<br>UNCLASSIFIED | 1b. RESTRICTIVE MARKINGS<br>N/A |
| 2a. SECURITY CLASSIFICATION AUTHORITY<br>N/A | 3. DISTRIBUTION/AVAILABILITY OF REPORT<br>Approved for public release; distribution unlimited. |
| 2b. DECLASSIFICATION/DOWNGRADING SCHEDULE<br>N/A | |
| 4. PERFORMING ORGANIZATION REPORT NUMBER(S)<br>N/A | 5. MONITORING ORGANIZATION REPORT NUMBER(S)<br>RADC-TR-84-142 |
| 6a. NAME OF PERFORMING ORGANIZATION<br>Stanford University<br>6b. OFFICE SYMBOL (If applicable) | 7a. NAME OF MONITORING ORGANIZATION<br>Rome Air Development Center (EEA) |
| 6c. ADDRESS (City, State and ZIP Code)<br>W.W. Hansen Laboratories of Physics<br>Stanford CA 94305 | 7b. ADDRESS (City, State and ZIP Code)<br>Hanscom AFB MA 01731 |
| 8a. NAME OF FUNDING/SPONSORING ORGANIZATION<br>Rome Air Development Center<br>8b. OFFICE SYMBOL (If applicable)<br>EEA | 9. PROCUREMENT INSTRUMENT IDENTIFICATION NUMBER<br>F19628-83-K-0011 |
| 8c. ADDRESS (City, State and ZIP Code)<br>Hanscom AFB MA 01731 | 10. SOURCE OF FUNDING NOS.<br>PROGRAM ELEMENT NO. 61102F; PROJECT NO. 2305; TASK NO. J5; WORK UNIT NO. 32 |

11. TITLE (Include Security Classification)
TEMPERATURE COMPENSATION OF SURFACE TRANSVERSE WAVES FOR STABLE OSCILLATOR APPLICATIONS

12. PERSONAL AUTHOR(S)
B. A. Auld

| 13a. TYPE OF REPORT | 13b. TIME COVERED | 14. DATE OF REPORT (Yr., Mo., Day) | 15. PAGE COUNT |
|---|---|---|---|
| Interim | FROM Mar 83 TO Mar 84 | June 1984 | 28 |

16. SUPPLEMENTARY NOTATION
N/A

| 17. COSATI CODES | | |
|---|---|---|
| FIELD | GROUP | SUB. GR. |
| 08 | 01 | |
| 07 | 02 | |

18. SUBJECT TERMS (Continue on reverse if necessary and identify by block number)
Surface Transverse Waves (STW); Delay Lines; Surface Acoustic Waves (SAW); Resonators; Temperature Compensation; (Continued on reverse)

19. ABSTRACT (Continue on reverse if necessary and identify by block number)

This research is concerned with methods for achieving temperature compensation of surface-type acoustic wave resonators and delay lines in high coupling materials such as lithium niobate and lithium tantalate. Emphasis is placed on surface transverse waves (STW) - that is, horizontally polarized shear waves trapped on the surface by a grating structure consisting of grooves, mass loading strips, conducting strips, or combinations thereof. For delay line applications operation is in the passband of the grating, for resonator applications two gratings are required - a passband grating for the standing wave and a stopband grating for the reflectors. An analysis of the temperature coefficient of delay has been developed and programmed for STW propagating normal to the X-axis in rotated Y-cut trigonal crystals. Using this program it has been found that temperature compensation using a grooved grating alone can be achieved for these STW in lithium tantalate and lithium niobate and grating designs have been worked out. In this configuration the STW are, however, non-piezoelectrically active and an external transducer is required. To allow extension of

| 20. DISTRIBUTION/AVAILABILITY OF ABSTRACT | 21. ABSTRACT SECURITY CLASSIFICATION |
|---|---|
| UNCLASSIFIED/UNLIMITED ☐ SAME AS RPT. ☒ DTIC USERS ☐ | UNCLASSIFIED |

| 22a. NAME OF RESPONSIBLE INDIVIDUAL | 22b. TELEPHONE NUMBER (Include Area Code) | 22c. OFFICE SYMBOL |
|---|---|---|
| Paul H. Carr | (617) 861-3686 | RADC (EEA) |

DD FORM 1473, 83 APR EDITION OF 1 JAN 73 IS OBSOLETE.

UNCLASSIFIED
SECURITY CLASSIFICATION OF THIS PAGE

this new temperature compensation technique to arbitrary crystal orientations, a more general grating theory is being developed. This will allow grating temperature compensation to be investigated for both SAW and quasi-STW. Grating designs will be developed in the coming year.

Item 17 (Cont'd).

| Field | Group |
|---|---|
| 17 | 04 |

Item 18 (Cont'd).

Gratings
Lithium Tantalate
Lithium niobate
TCD
Surface Skimming Bulk Waves (SBAW)

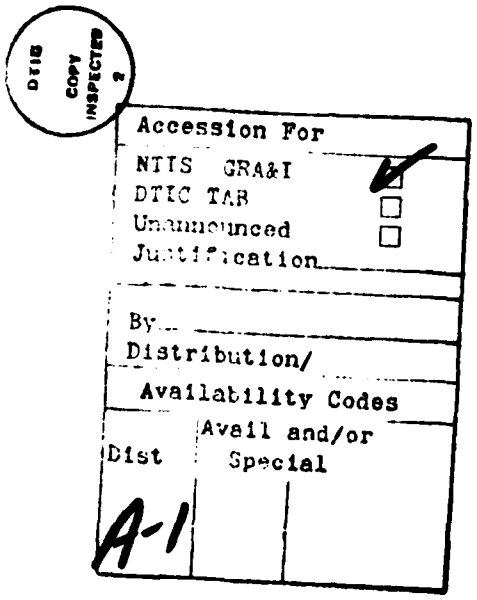

# I. INTRODUCTION AND GENERAL BACKGROUND

Surface acoustic waves (SAW) have, for more than ten years, played an increasingly important role in electronics technology, especially signal processing in the VHF-UHF frequency ranges. The initial emphasis in SAW research and development was on tapped delay lines, for which the planar geometry of a SAW structure is particularly well-suited. As the theory and practice of SAW transducers became more and more sophisticated, delay lines were tailored for chirp transform processing and wide-band frequency selection filters. The extension of SAW technology into the microwave region bridged a gap between the range of previously existing acoustics techniques and that covered by the newly emerging magnetostatic wave (MSW) technology at even higher microwave frequencies.

During the 1980's and beyond there will be a need for low cost, low noise oscillator circuitry in high frequency communications systems such as the Global Position Satellite Navigation system. Current performance of SAW oscillators now allows their use in civil communication systems, especially in digital radio links. Typical applications include shift oscillators, carrier and bit timing recovery circuits, and pilot generators. Other applications requiring highly stable VHF-UHF oscillators are spectrum analysers, gas sensors, and RF converters. Because of this emphasis on narrow-band oscillator operation, new temperature compensated materials and techniques are now being actively investigated. Both long- and short-term stability in SAW oscillators has become important to the success of these signal processing systems and of other applications.

In 1976–77 two new, and related, developments occurred in surface wave acoustics: (1) horizontally polarized shear (SH) grating surface waves,[1] and (2) shallow bulk acoustic (SBAW), also called surface-skimming bulk acoustic (SSBW), waves.[2] By contrast with the Rayleigh wave propagation used in SAW technology, these new phenomena are concerned with shear motion polarized parallel to the substrate surface. A smooth surface cannot support an SH-type of surface wave, but it was demonstrated theoretically and experimentally that this type of surface wave does exist on a periodically perturbed surface.[1] These waves have the potential advantage of a longer wavelength and hence higher operating frequency, and a better frequency-temperature characteristic. Initial results with SH wave devices revealed

prohibitively high insertion losses. By incorporating a shallow grating between transducers it was found that the losses could be reduced to, typically, 10 dB.[3] The grating trapped and guided the wave along the surface and reduced diffraction, which was the cause of the high insertion loss. This effect, which can be explained by a straightforward space harmonic analysis of gratings on isotropic substrates, was exploited in fabricating delay line oscillators operating at frequencies as high as 2 and 3.4 GHz[3,4]

Oscillators controlled by surface acoustic waves (SAW), rather than STW, are of both delay line and resonator types. A SAW resonator consists of a pair of metallic or grooved grating reflectors spaced at a resonant length for frequencies within the grating stop band and excited by an internal IDT. Incorporation of such structures in an oscillator circuit provides increased selectivity and stability. For SAW applications, three types of grating reflectors have been studied and utilized: (1) etched grooves, (2) mass-loading deposited electrode strips, and (3) short-circuiting deposited metallic strips. Type I gratings provide the highest $Q$ but are the most difficult to fabricate; Type II gratings provide satisfactory $Q$ and are somewhat easier to fabricate; and Type III gratings are the simplest to fabricate but have adequate reflectivity only on strongly piezoelectric substrates ($LiNbO_3$ and $LiTa0_3$).[5] Another consideration in stable resonator design is the need for crystal cuts having minimal changes in SAW velocity with temperature. Unfortunately, the strong piezoelectric coupling materials that permit use of shorting strip gratings (and are also more satisfactory for the IDT design) do not have zero temperature coefficient crystal cuts. For this reason SAW oscillators requiring the utmost frequency stability use rotated Y-cut quartz substrates of various types (AT,ST). Studies are currently being made of doubly rotated cuts, such as the SC cut. Deposition of layers on the substrate are known to change the temperature curve of AT quartz and this has been proposed as a method for adjusting the temperature compensation.

The attraction of SSBW and STW in delay line and resonator applications is due to: (1) Higher acoustic velocities, leading to larger IDT periodicities at the same frequency; (2) Lower propagation loss for certain orientations of quartz and berlinite; and (3) Smaller temperature coefficients of delay in quartz and berlinite. The crystal cuts of interest are rotated-Y cuts, with the propagation direction normal to that for SAW. Delay line filters of SSBW type have also been constructed

on rotated cuts of $LiTaO_3$, having large $k^2$ and satisfactory temperature stability for certain applications. However, no completely temperature-compensated SSBW cuts have been discovered for $LiNbO_3$ or $LiTaO_3$, which prevents use of these attractive materials in highly stable delay line oscillators controlled by SSBW. In the case of resonator-controlled oscillators, SSBW suffer from a diffraction limited $Q$, due to the fact that SSBW are not guided surface waves. Improvement in the performance of SSBW delay lines due to deposition of a metallic periodic grating that traps the energy on the surface has been calculated and observed experimentally. In view of the results presented in the literature concerning the adjustment of SAW temperature compensation by a mass-loading overlay, these energy trapping gratings will also change the temperature compensation of the STW trapped by the grating. For grooved gratings the effect should be even more pronounced, because the STW velocity is determined not only by the material properties but also by the topography of the grating profile. The major goal of this proposed study of STW propagation is to investigate these multiple compensation effects and, in particular, to look for combinations of crystal orientation, mass loading, groove topography and metal shorting capable of realizing a zero TCD on $LiNbO_3$ and $LiTaO_3$. Since multi-compensation effects are known to occur in SC-cut crystals, where stress-compensation also occurs, another interesting direction for this project will be to look for STW cuts and grating geometries having properties similar to those of the SC-cut.

The analysis of STW in Reference 1 dealt with deep gratings at low frequencies on isotropic material surfaces, and the calculations were based on published treatments of the analogous electromagnetic problem using the space harmonic method. For the high frequency structures of interest in connection with the VHF-UHF oscillators, shallow gratings are indicated and one is led to use a perturbation approach in treating the effect of the grating teeth on the surface boundary conditions. The perturbation technique is most generally useful since it can be easily applied to the anisotropic case and appears to offer possibilities for the inclusion of piezoelectricity. It uses Tiersten boundary conditions for the perturbation of a substrate by a thin surface layer in order to analyze the fields within the grating teeth, a method that has recently been extended to take correctly into account the boundary conditions on the edges of the teeth.[5]

Several rigorous analyses have recently been reported for deep gratings on isotropic substrates.[7,8] Practical grating structures, however, will necessarily be used on crystal substrates that are both anisotropic and piezoelectric, where perturbation is the *only* analytical technique applicable. This is not a serious limitation, since resonator structures require weak gratings many periods in length—a case suitable for perturbation treatment. This has been developed for the important practical case of rotated Y-cut trigonal crystals (quartz, berlinite, $LiNbO_3$ and $LiTaO_3$) and numerical results have been calculated for quartz and berlinite.[9] The analysis allows the effect of anistropy on STW gratings to be obtained directly from the material parameters, unlike the case of SAW gratings (where the theory of grooved gratings has been based on empirical considerations[10]).

Grating reflectors for SAW resonators are designed by applying the empirically-based infinite grooved grating theory to develop the wave transmission matrix representation of a grating of finite length. This permits calculation of the grating reflector length from the depth of the grooves. With a similar matrix representation of the standing wave region between the reflectors, this leads to a complete resonator design, as in the reference cited. In Reference 9 an analogous finite length grating theory was developed for STW, and transmission measurements on AT quartz showed good agreement with theory. For STW resonators, both the reflectors and the standing wave region between must have grooved surfaces; and the reflector and resonator gratings must be designed so as to avoid diffraction into bulk waves at the boundary. General resonator design criteria based on this concept are presented in Reference 11.

## II. WORK STATEMENT FOR FIRST 12-MONTH PERIOD

Tasks 1 and 2—to be performed during first twelve months of the contract:

Task 1 Develop and evaluate for various materials a temperature perturbation analysis of TCD for grooved STW on rotated Y-cut trigonal crystals.

Task 2 Make a quantitative estimate of the degree of temperature compensation achievable with a grooved structure, to determine the likelihood of achieving zero temperature coefficient with choice of groove shape only.

## III. PROGRESS DURING FIRST 12-MONTH PERIOD

### (a) Temperature Compensation of Pure STW on Rotated Y-cut Trigonal Crystals

In this case, pure STW occur only for propagation normal to the X-axis . This geometry was treated in Reference 9, where the basic wave theory was developed. The analysis considered propagation on corrugated surfaces of rotated Y-cut trigonal class crystals (quartz and berlinite) with grating dimensions corresponding to the cavity region of Fig. 1, where $W = \Lambda/2$. The method used was to apply Floquet's Theorem, which gives the general form of the characteristic wave solutions, separately to the semi-infinite substrate and to the grating. Application of appropriate boundary conditions at $Y = 0$ then gives the dispersion relation and the relative amplitudes of the various space harmonics. The method used in applying the boundary conditions was to assume a shallow grating and then calculate the stress at the bottom of a tooth using the Datta-Hunsinger Perturbation Formula.[6] To calculate the dispersion curves, a small frequency perturbation $\delta\omega$ and a small propagation constant perturbation $\delta\beta$ were assumed relative to the Bragg frequency crossover (Fig. 2), leading to the coupled wave dispersion relation

$$\delta\beta^2 = (\delta\omega/V_s)^2 - K^2 \quad , \tag{1}$$

where the surface skimming bulk wave (SSBW) velocity is

$$V_s^2 = (C_{56}C_{66} - C_{56}^2)/\rho C_{66} = C_{eff}/\rho \quad ,$$

the space harmonic coupling constant is

$$K = \frac{2(\pi)\rho V_s^2}{\Lambda C_{66}}(h/\Lambda)^2 \quad ,$$

and

$h$ is the height of the grating
$\Lambda$ is the period of the grating
$\rho$ is the density of the crystal
$C_{xx}$ are the crystal stiffness constants.

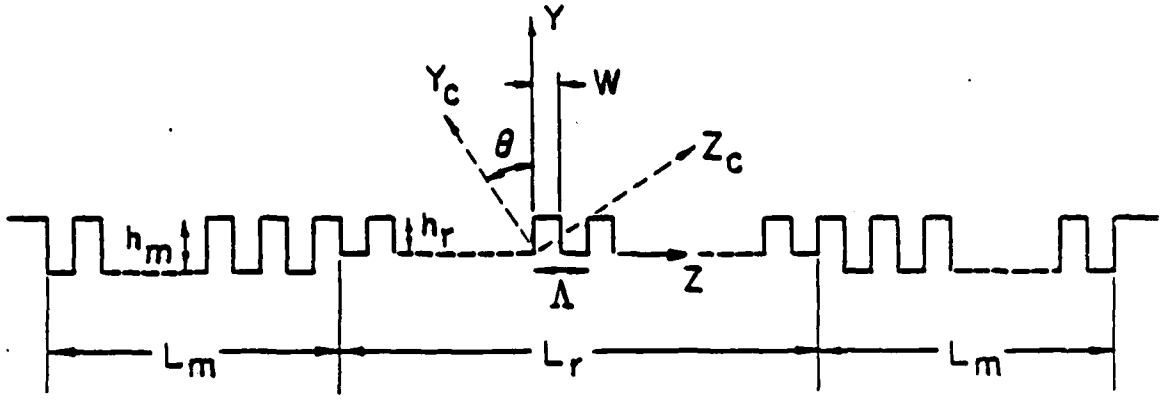


**FIGURE 1**

Definition of parameters for an STW grating resonator. The central region is in a grating passband.

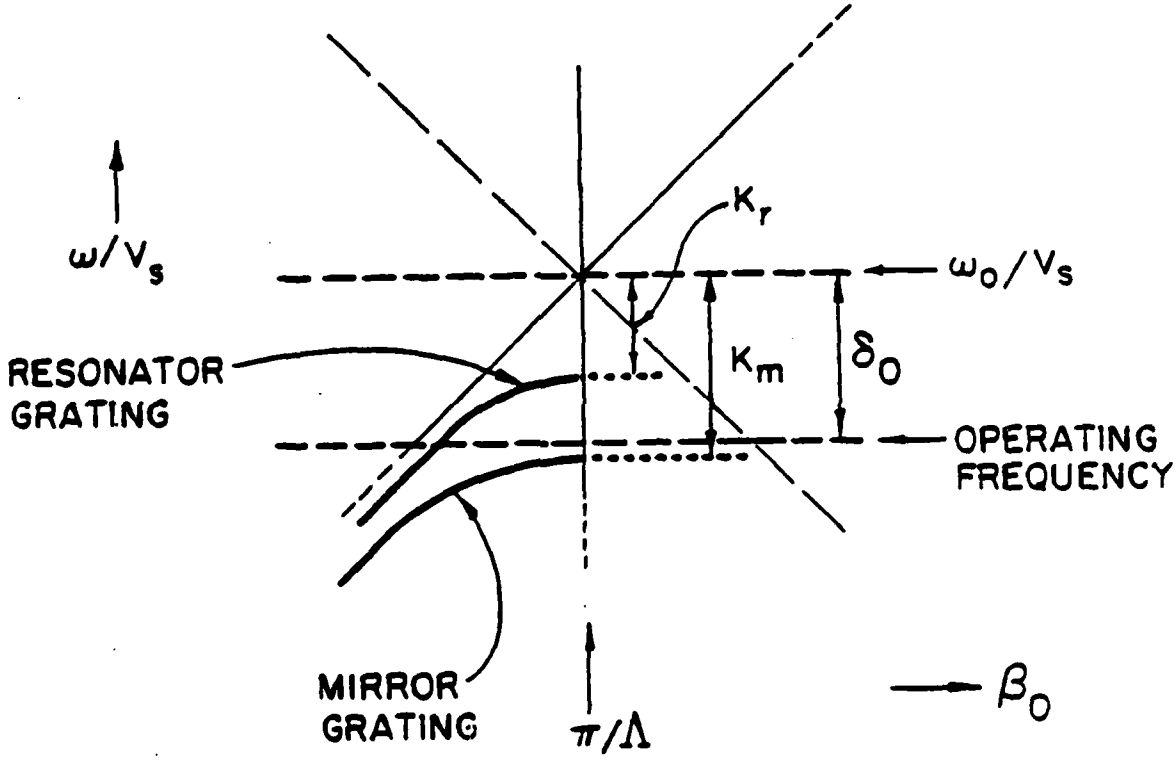


**FIGURE 2**

Dispersion curves for the resonator and mirror gratings of Fig. 1 near the first stop band.

Using the above results, the velocity for pure STW propagation on corrugated rotated Y-cut trigonal crystals can be calculated. The result is

$$V_{stw} = \frac{V_s \omega}{\omega_0 - [(\omega_0 - \omega)^2 - (V_s K)^2]^{1/2}} \quad , \tag{2}$$

where the Bragg, or center stop band, frequency is

$$\omega_0 = \pi V_s / \Lambda \quad ,$$

and the STW frequency is $\omega$. This equation is valid for all trigonal crystals, including quartz, berlinite, lithium tantalate and lithium niobate. To have a propagating STW the operating frequency must be below the lower edge of the stop band (Fig. 2). That is, we must satisfy the following condition in order to have a real STW velocity,

$$(\omega_0 - \omega)^2 > (V_s K)^2 \quad . \tag{3}$$

Since the temperature and rotation angle dependence of $V_s$, $\omega_0$, and $K$ can be obtained from the temperature dependence of the material constants and grating dimensions, the temperature dependence of the STW velocity can be calculated. To investigate temperature-compensation effects it is necessary to first consider the first-order temperature coefficient of the phase delay (TCD). This is defined as[12]

$$\text{TCD} = \alpha - (1/V_{stw}) \frac{dV_{stw}}{dT} \quad , \tag{4}$$

where $\alpha$ is the linear expansion coefficient in the direction of wave propagation. A computer program was developed, using Eq. (1) and Eq. (4) to plot $V_{stw}$ and TCD *vs.* temperature. The purpose of the program is to provide a check on predictions of a zero crossing of the TCD curve, as well as to act as a guide in finding a temperature range over which the TCD will be close to zero. This program is very general and can be used to estimate STW velocity and TCD (neglecting piezoelectricity) for any rotated Y-cut trigonal crystal (quartz, berlinite, niobate or tantalate).

To better facilitate the prediction of a zero TCD crossing, a scheme was developed for relating the TCD curves to the crystal rotation angle, with the grating dimensions and operating frequency as parameters. If only small changes with temperature are considered and lower order terms are neglected whenever possible,

the TCD can be approximated by

$$\mathrm{TCD} = \frac{H[2(V_{stc} - \Lambda_{tc}) - C_{66tc} + 2h_{tc} + \rho_{tc}] - J[V_{stc} - \Lambda_{tc}]}{F_o - F_o^2} \quad , \tag{5}$$

where

$$H = 4(h/\Lambda)^4 (C_{eff}/C_{66})^2$$
$$J = \omega/\omega_0 - (\omega/\omega_0)^2$$
$$F_0 = \left[(1 - \omega/\omega_0)^2 - H\right]^{1/2}$$

$V_{stc}$ and $C_{66tc}$ are the surface skimming wave velocity and 66 stiffness temperature coefficients in the rotated coordinates;

$\Lambda_{tc}$ and $h_{tc}$ are the linear expansion coefficients for the period and height in the rotated coordinates;

$\rho_{tc}$ is the temperature coefficient of density of the crystal

This expression can be evaluated, since the temperature coefficients for $C_{66}$, $h$ and $\rho$ have been found experimentally[13,14] and the skimming bulk wave velocity temperature coefficient is calculated to be

$$V_{stc} = \frac{C_{56}C_{55tc} - C_{56}^2/C_{66}(2C_{56tc} - C_{66tc})}{2C_{eff}} - \rho_{tc}/2 \quad .$$

This equation for the surface skimming bulk wave velocity temperature coefficient was checked by substituting the stiffness constants for quartz[14] and comparing to published curves for the SSBW temperature coefficient.[15] Our curves matched the published curves exactly.

Setting the TCD (Eq. 5) equal to zero gives the condition on the frequency, rotation angle and grating dimensions required to achieve a TCD zero crossing. This condition is

$$J = HA \quad , \tag{6}$$

where $J$ and $H$ are defined above and the compensation factor $A$ is

$$A = \left[2 + \left(\frac{2h_{tc} + \rho_{tc} - C_{66tc}}{V_{stc} - \Lambda_{tc}}\right)\right] \quad .$$

This compensation factor is a measure of the ability to compensate a given crystal cut using the grating structure under investigation. The greater the compensation factor the smaller the height of the grating required to achieve a zero crossing. If

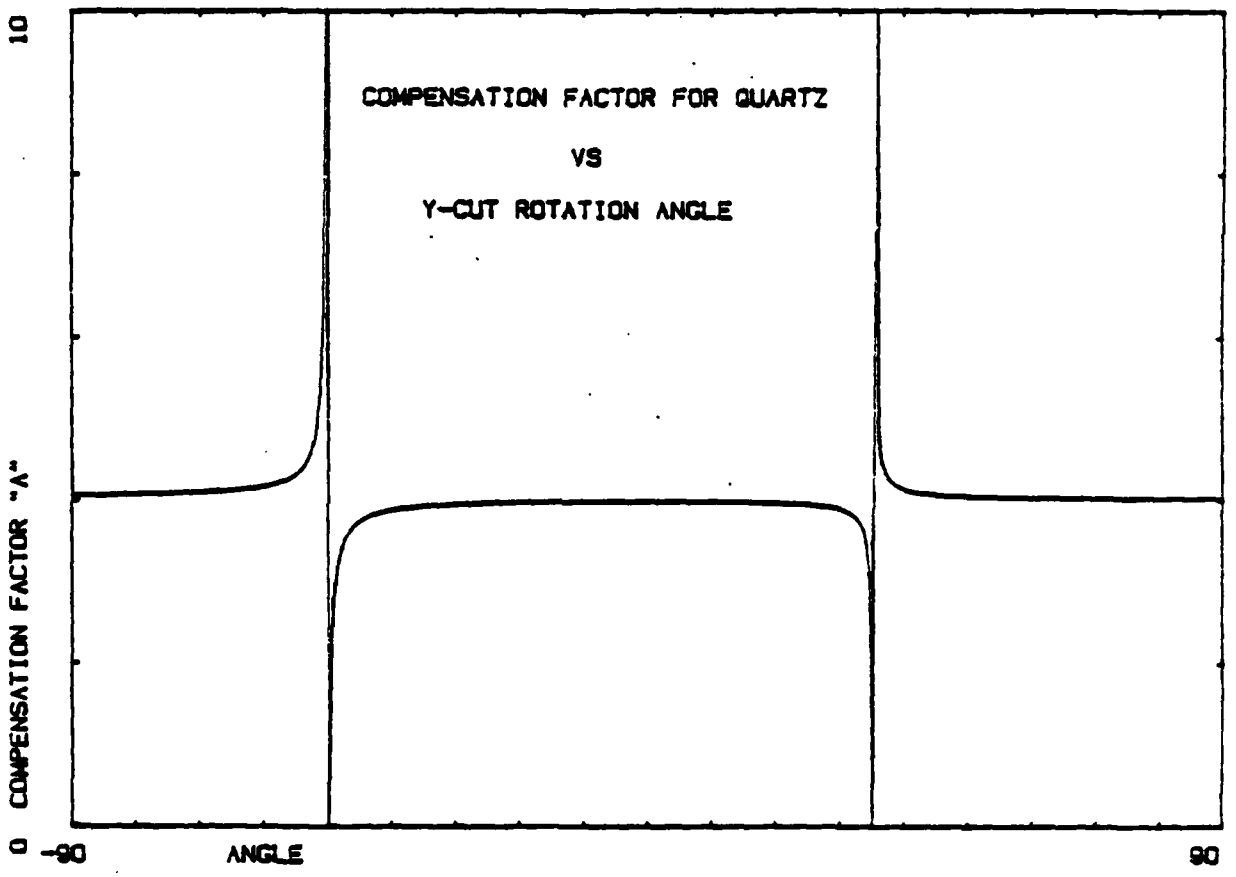


## FIGURE 3

Compensation factor A (Eq. 8) versus Y-cut rotation angle for quartz. Grating compensation is possible only for A greater than zero (-90° to -50°, -49° to 35°, 35° to 90°). Room temperature.

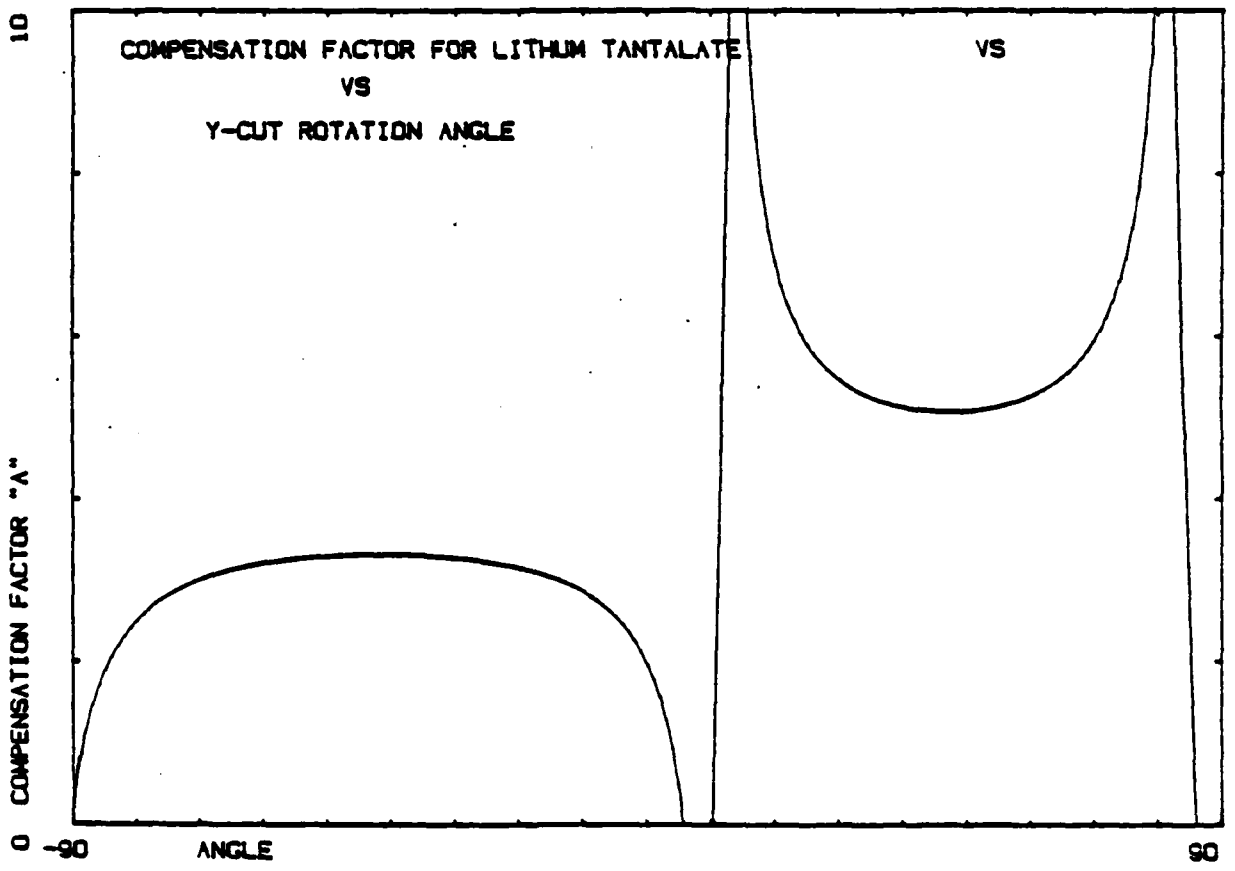


**FIGURE 4**

As in Fig. 3. for lithium tantalate (-90° to 5°, 12° to 33°.)

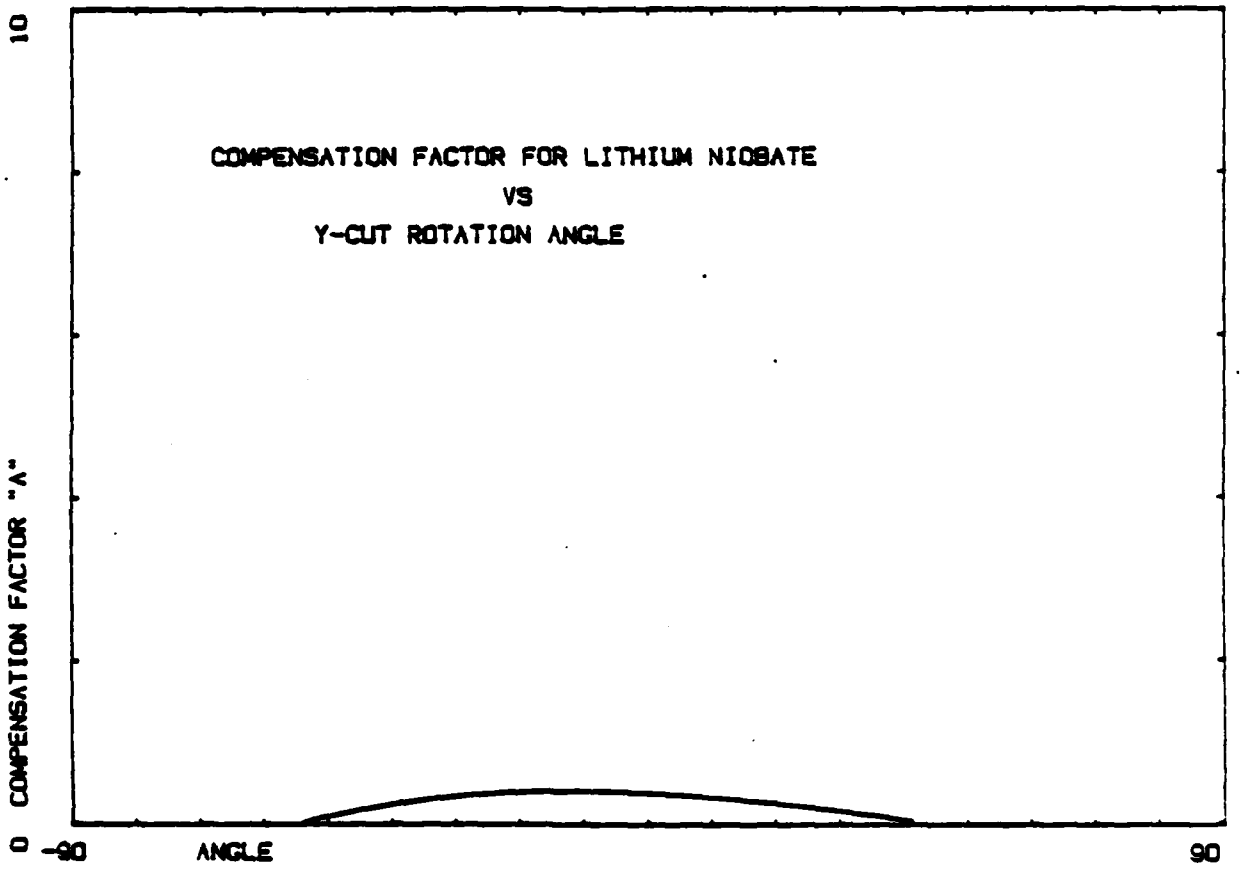


**FIGURE 5**

As in Fig. 4. for lithium niobate (-54° to 41°.)

the compensation factor is negative the crystal cut cannot be compensated using this kind of grating, because the addition of the grating increases the TCD, thus making the temperature compensation worse. Compensation factors versus Y-cut rotation angle are given for quartz in Fig. 3, lithium tantalate in Fig. 4, and lithium niobate in Fig. 5.

The above theory shows that a compensation factor of 4 at a frequency of 1 GHz corresponds to a Bragg frequency of 1.3 GHz, a grating period of 1.5 microns and a grating depth of 0.48 microns for quartz and lithium tantalate. A shallow grating was assumed, which implies that the grating depth is much smaller than the wavelength of the STW. The wave lengths at 1 GHz of the STW were 2.8 microns for tantalate and 3.7 microns for quartz. Therefore the assumption is reasonable and indicates that complete temperature compensation of quartz or lithium tantalate with a grating of this type should be realizable. However, in the case of lithium niobate the maximum compensation factor is approximately 0.37 at an angle of -15°. This small compensation factor requires an operating frequency of 1 GHz, a Bragg frequency of 3.8 GHz, a grating depth of about 0.29 microns, and a grating period of 0.5 microns. Because the operating frequency is far below the Bragg frequency, our coupled wave approximation to the theory (small $\delta\omega$) may not predict with complete accuracy the required grating depth. However, compensation does occur for niobate and more accuracy can be achieved by retaining more terms in the Floquet expansion. This straightforward modification should then permit accurate prediction of the grating depth required for zero TCD at room temperature.

To implement this more accurate calculation, it is necessary to relax the assumption that the operating frequency is close to the Bragg frequency. Recall that a small $\delta\omega$ and a small $\delta\beta$ about the stopband were assumed, to simplify the dispersion relation. Relaxing this assumption leaves a dispersion relation which can only be solved numerically. These calculations are more tedious but will confirm the accuracy of the approximate dispersion relation above, as well as giving the true behavior of the dispersion relation in a region far below the stopband. This is important because design of temperature compensated delay lines may be more practical in this low frequency region. These extended calculations will also give the true dispersion relation in the region above the Bragg frequency, which is of considerable theoretical interest and is not correctly predicted by our present theory.

Piezoelectric effects for pure X-polarized STW on rotated Y-cut lithium niobate and lithium tantalate, have also been examined. There is no piezoelectric stiffening of rotated Y-cut trigonal 3 m crystals. Thus piezoelectricity has no effect on the rotated Y-cut STW. However, the lack of piezoelectric stiffening makes it impossible for an IDT to couple to a pure STW on rotated Y-cut lithium niobate or tantalate. Because of this coupling problem it is necessary to use an intrinsic transducer scheme to make use of the compensation properties of pure STW on these substrates. One such scheme would involve depositing a thin layer of ZnO on the surface of the crystal before putting down the metal fingers of the IDT. The added cost due to extra processing as well as the loss in coupling efficiency makes such a scheme rather impractical.

### (b) Temperature Compensation of Pure STW on Gallium Arsenide

Because of the extremely attractive properties of gallium arsenide for fast semiconductor devices, the possibility of realizing integrated semiconductor-acoustic devices on gallium arsenide substrates is arousing considerable current interest. For this reason a first evaluation has been made of the possibilities for temperature compensated STW propagation on this substrate. Equation (2) can be applied to STW propagation in the cube diagonal plane of gallium arsenide with a slight modification to the surface skimming bulk wave velocity term ($V_s$) and the space harmonic coupling constant term ($K$). In this case

$$V_s^2 = (C_{44}C_{66} - C_{46}^2)/\rho C_{66} = C_{eff}/\rho$$

and

$$K = 2(\pi)h^2/(\Lambda)^3 \quad .$$

Similar results are obtained for STW propagation in a cube face. A modified version of the TCD computer program has also been developed for these cuts of gallium arsenide, the only ones permitting pure STW.

Results of computer evaluation of the compensation factor show that, for STW propagation in the cube face, it is equal to zero for all propagation directions, a conclusion expected from the elastic isotropy of gallium arsenide in the cube face. The compensation factor for STW propagation in the cube diagonal plane of gallium arsenide is never greater than zero, so that a zero TCD crossing cannot be achieved.

The smallest TCD value calculated was for the surface skimming bulk wave (that is, an STW with no grating), which had a value of 37 ppm. The negative compensation factor indicates that addition of a grating increases the TCD, a result confirmed by numerical evaluation of the TCD formula for gallium arsenide. However, the literature does give designs of temperature stable gallium arsenide surface acoustic wave delay lines.[12] In this reference it is shown numerically that a SAW can be completely temperature-compensated by adding a double layer of gold and silicon dioxide to the gallium arsenide. This suggests that it will be possible to temperature-compensate SAW propagation with a grating designed according to the generalized surface grating wave theory outlined in (d) below.

### (c) Propagation of Quasi-STW along the X-axis of Rotated Y-cut Trigonal Crystals

A more attractive approach than the development of special transducers for pure STW (discussed at the end of subsection (a)) is to choose a propagation direction that *can* couple to an IDT. One such propagation direction is along the X-axis of rotated Y-cut lithium tantalate or lithium niobate. Propagation in this direction is by quasi-STW, already described in the literature.[16] Resonators using this type of surface transverse wave on 49° rotated Y-cut, X-propagation lithium niobate have been reported by Zhang *et al.*[17] The quasi-STW wave problem is much more complicated because one must allow for an arbitrary displacement polarization, while in the pure STW case the polarization is in one-dimension only. Treatment of an arbitrary polarization displacement requires a complete redevelopment of grating theory from first principles. Such a theory, described in the following subsection, gives a quantitative method for calculating not only pure STW grating waves but also Rayleigh and pseudosurface grating waves. This is a major advance because it allows SAW resonator gratings, now designed from experimentally determined parameters, to be analyzed directly from the material properties of the substrate. It also opens the way to temperature-compensating SAW on lithium niobate and lithium tantalate by means of gratings operating in the passband. This possibility of temperature-compensating SAW, as well as STW, raises the question of the relative advantages of these two types of waves. Recall that, for quartz, STW is favored over SAW because it has a significantly

greater velocity, which eases the problem of mask fabrication at higher frequencies. However, it has been reported in the literature that for lithium niobate and lithium tantalate the SAW and bulk shear wave velocities are approximately the same, so that the advantage of SSBW and STW in facilitating mask fabrication in these materials is lost. Because of this, it is felt that the potential for temperature-compensating surface waves with gratings is just as important for SAW as it is for STW. The choice will depend on which gives the better performance.

### (d) Theory of Generalized Surface Grating Waves

In rotated Y-cut trigonal crystals, surface skimming bulk waves (SSBW) exist only for propagation normal to the X-axis. Addition of a surface grating converts these skimming bulk shear waves into pure shear (or transverse) *surface* waves (STW). As noted above, temperature-compensation of these waves on quartz, lithium niobate, and lithium tantalate can be achieved by choosing the crystal orientation and the grating dimensions. In the cases of lithium niobate and lithium tantalate, however, these are not piezoelectrically active, and cannot be excited with an IDT. Piezoelectric coupling is obtained for propagation along the X-axis of rotated Y-cut lithium niobate and lithium tantalate. However, for this direction of propagation pure SSBW and STW exist only for certain specific rotation angles. Consequently, to study temperature compensation of surface grating waves on piezoelecrically active cuts it is necessary to extend the previous theory (developed for pure shear waves, polarized parallel to the crystal surface) to the case of general polarizations.

Two approaches are being followed:

#### (i) Perturbation Theory

This approach is applicable to rotated Y-cut orientations having an X-propagating plane shear wave solution with polarization very nearly parallel to the crystal surface for a certain angle of rotated Y-cut lithium tantalate.[16] In this situation one can approximate the actual rotated stiffness matrix by a hypothetical matrix having a pure shear SSBW solution, plus a small perturbation. A pure STW solution is found, using the hypothetical matrix, and the velocity is then modified by perturbation theory[18] according to the small difference between the actual and

hypothetical stiffness matrices.

### (ii) Generalized Floquet Theory

If the crystal cut does not permit an approximately pure STW solution, the grating wave theory must be completely reformulated from the beginning. This has been done in the manner summarized below. Important consequences of this breakthrough are: (1) it permits a thorough investigation of grating temperature compensation in gallium arsenide, where compensation has been found to be impossible for pure STW crystal orientations; (2) it provides the first development from fundamentals (rather than experiment-based empirical models) of SAW grating theory and therefore opens up the highly important technological area of termperature-compensation for SAW gratings; and (3) it makes possible an in-depth study of surface trapping of pseudosurface waves and leaky waves on arbitrarily oriented crystals. To simplify the discussion, it will be restricted here to crystal cuts, such as rotated Y-cut lithium niobate with propagation normal to the X-axis, for which both SSBW and saggital plane SAW exist. In the case of lithium niobate the saggital plane SAW is piezoelectrically active and, indeed, is a commonly used orientation in practice. For this simplified discussion, piezoelectric effects will be ignored.

Figure 1 defines the grating parameters. Attention will be focused here on the passband grating in the center of the figure. In the theory of pure STW the particle displacement is in the X-direction only. Floquet theory is applied by: (1) expanding the acoustic field in the substrate ($Y < 0$) in terms of space harmonics. (2) developing the field in the teeth by means of Datta-Hunsinger perturbation theory, (3) matching boundary conditions at $Y = 0$, to obtain the characteristic equation, and (4) invoking the coupled wave approximation to obtain a closed-form solution for shallow gratings.[9] As an example of the generalized theory, this same approach will be applied here to SAW grating waves on an isotropic substrate. This is for illustrative purposes only. The general format is the same for SAW propagating normal to X on rotated Y-cut lithium niobate, and this case will be pursued quantitatively during the next quarter.

As in standard SAW analysis the field in the substrate is expressed as a superposition of longitudinal and vertical shear partial waves. For grating wave theory

each of these types of partial waves is a sum over an infinity of space harmonics. The $n^{th}$ space harmonics of the two types of partial waves are defined as

$$\begin{aligned} u &= \dot{u}_{nL} e^{\alpha_{nL} Y} e^{-i\beta_{nL} Z} \\ u &= \dot{u}_{nS} e^{\alpha_{nS} Y} e^{-i\beta_{nS} Z} \end{aligned} \quad , \tag{7}$$

where the polarization vectors $\dot{u}$ (containing $Y$ and $Z$ components only) are of longitudinal and shear types, such that

$$\begin{aligned} -\alpha_{nL}^2 + \beta_{nL}^2 &= (\omega/V_\ell)^2 \\ -\alpha_{nS}^2 + \beta_{nS}^2 &= (\omega/V_s)^2 \end{aligned} \quad . \tag{8}$$

Also, the space harmonic propagation factor is defined as

$$\beta_n = \beta_o + 2\pi n/\Lambda \quad . \tag{9}$$

For $n = 0$, Eqs. (7) and (8) reduce to the partial waves used in analyzing SAW propagation on a smooth surface.

The boundary conditions at $Y = 0$ in Fig. 1 involve the field components $u_Y$, $u_Z$, $T_{YY} = T_2$, and $T_{ZY} = T_4$. After evaluation of the 2 and 4 stresses for each space harmonic, Eq. (7), the total boundary fields (at $Y = 0$) are found to be described by the two matrix equations

$$\begin{bmatrix} u_Y \\ u_Z \end{bmatrix} = \sum_{n=-\infty}^{\infty} \begin{bmatrix} u_{YL} & u_{YS} \\ u_{ZL} & u_{ZS} \end{bmatrix}_n \begin{bmatrix} a_{nL} e^{-i\beta_{nL} Z} \\ a_{nS} e^{-i\beta_{nS} Z} \end{bmatrix} \tag{10}$$

$$\begin{bmatrix} T_2 \\ T_4 \end{bmatrix} = \sum_{n=-\infty}^{\infty} \begin{bmatrix} T_{2L} & T_{2S} \\ T_{4L} & T_{4S} \end{bmatrix}_n \begin{bmatrix} a_{nL} e^{-i\beta_{nL} Z} \\ a_{nS} e^{-i\beta_{nL} Z} \end{bmatrix} \quad , \tag{11}$$

where $a_{nL}$ is the amplitude of the $n^{th}$ longitudinal space harmonic and $a_{nS}$ is the amplitude of the $n^{th}$ shear space harmonic. The meaning of these equations can be clarified by noting that they are both scalar equations for $u_X$ and $T_{XY} = T_6$ in the pure STW case. Furthermore, in the case of a SAW on a smooth surface only the $n = 0$ space harmonic exists, and the stresses are zero on the left-hand side of Eq. (11). This gives

$$0 = \begin{bmatrix} T_{2L} & T_{2S} \\ T_{4L} & T_{4S} \end{bmatrix}_0 \begin{bmatrix} a_{oL} \\ a_{oS} \end{bmatrix} \tag{12}$$

Setting the determinant of the matrix equal to zero should give the characteristic equation for a Rayleigh wave on an isotropic substrate, and this has been verified.

For a grating wave the fields in Eqs. (10) and (11) must be matched to the fields in the teeth by using Datta-Hunsinger perturbation theory, just as in the case of STW; but matrix equations are now obtained, rather than scalar equations. In this case, the Datta-Hunsinger relations for the stresses under the teeth are

$$\begin{bmatrix} T_2 \\ T_4 \end{bmatrix} = \begin{bmatrix} D_{2Y} & 0 \\ 0 & D_{4Z} \end{bmatrix} \begin{bmatrix} u_Y \\ u_Z \end{bmatrix} , \tag{13}$$

with the displacements given by Eq. (10). Between the teeth the stresses are zero. Substitution of these results into the left-hand side of Eq. (11) leads to coupling among the space harmonic amplitudes. This relation is a two-dimensional matrix equation analogous to the scalar equation found for pure STW. As in that case, an infinite set of linear equations in the space harmonic amplitudes is obtained by multiplying with

$$e^{i\beta_m Z}$$

and integrating with respect to $Z$ over one period of the grating . Because of the orthogonality of the exponential functions over a grating period, this yields equations of the form

$$\Lambda \begin{bmatrix} T_{2L} & T_{2S} \\ T_{4L} & T_{4S} \end{bmatrix}_m \begin{bmatrix} a_{mL} \\ a_{mS} \end{bmatrix} = \sum_{n=-\infty}^{\infty} [K_{mn}] \begin{bmatrix} a_{nL} \\ a_{nS} \end{bmatrix} , \tag{14}$$

for all values of $m$.

In the case of pure STW, the analogue of Eq. (14) is scalar and the coupled wave approximation is implemented by retaining only those values of $m$ for which the left-hand side is nearly zero at points close to the Bragg frequency (i.e., the so-called near-resonance terms). A difficulty arises in Eq. (14) because the left-hand side is a *matrix* and it is not clear how to apply the near-resonance condition. In fact, the matrix on the left-hand side of Eq. (14) is the $n^{th}$ space harmonic version of the matrix in Eq. (12). It therefore has zero determinant when the characteristic equation for SAW (i.e., SAW "resonance" conditions). This gives the clue for decoupling the amplitudes $a_{mL}$ and $a_{mS}$ on the left-hand side of Eq. (14), thereby allowing the coupled wave approximation to be implemented. Under SAW "resonance" conditions for the $m^{th}$ space harmonic the matrix on the left-hand side of Eq. (14) is a "null" matrix and has two identical eigenvectors. By taking this

eigenvector and a vector orthogonal to it as new basis vectors for the column matrix

$$\begin{bmatrix} a_{mL} \\ a_{mS} \end{bmatrix} ,$$

one can decouple Eq. (14) for space harmonics near the SAW "resonance" point. This gives scalar coupled wave equations for the 0 and -1 space harmonics of the SAW, with explicit expressions for the coupling induced by the grating, analogous to the equations used in calculating the dispersion curves and temperature-compensation of pure STW. With this new result it is possible to explicitly calculate from the material constants and the grating geometry the dispersion properties of SAW in the passband and stopband of a grating and to analyze temperature-compensation from the properties of the material. Similarly, a grating theory can be formulated for quasi-STW.

## IV. WORK STATEMENT FOR SECOND 12-MONTH PERIOD

Task 3 Look for temperature compensated gratings (involving grooves, mass loading and conduction effects) for $LiNbO_3$ and $LiTaO_3$.

Task 4 Develop a theory of conducting strip STW theory for planar surfaces of rotated Y-cut trigonal crystals and evaluate for various materials.

Task 5 Adapt Task 1 to mass loading STW.

Task 6 Develop theory of grooved STW to include complete and partial conductive coatings on rotated Y-cut trigonal crystals.

Task 7 Develop theory of grooved plus mass loading STW.

Task 8 Perform Task 3 in more detail.

## V. PLANS FOR SECOND YEAR

Research during the first year of this program (Section III. above) has already accomplished some of the goals set out in Task 3 of the second year work statement, namely to find temperature compensated gratings for $LiNbO_3$ and $LiTaO_3$. These results show that pure STW propagating normal to the X-axis on rotated Y-cut lithium niobate and lithium tantalate can be temperature-compensated with grooves alone. However, these waves were found to be piezoelectrically inactive, and pure

piezoelectrically active STW on gallium arsenide (investigated as an extra task) cannot be compensated with grooves alone.

These conclusions pointed to the need for a more general basic theory capable of treating grating surface waves other than pure STW—for example, the quasi-STW that propagates along the X-axis of rotated Y-cut lithium niobate and lithium tantalate. These are known to be piezoelectrically active, and some experimental results are available in the literature for propagation along a conductor-clad substrate. An approximate perturbation analysis of these waves was examined during the last quarter of the first year's effort. It has been concluded that this is not cost-effective because of the considerable effort required to generate results whose accuracy is not clearly defined. Consequently, it was decided to proceed with the exact treatment described in Section III(d).

Therefore, our plans for the first quarter of the second year are as follows:

(a) We will formulate a general theory of TCD for quasi-STW propagating along the X-axis, and SAW propagating normal to the X-axis of rotated Y-cut trigonal crystals.

(b) We will use (a) to find temperature-compensated designs for quasi-STW and SAW grooved gratings on rotated Y-cut trigonal crystals, selecting designs most suitable for experimental tests.

(c) We will adapt the results of (a) and (b) to mass loading gratings and gratings that combine grooves with mass loading.

## PUBLICATIONS

No publications were generated during this reporting period.

## PROFESSIONAL PERSONNEL

Professor B.A. Auld; D. Thompson, graduate student.

## INTERACTIONS

No presentations or interactions were made.

## REFERENCES


1. B.A. Auld, J.J. Gagnepain, and M. Tan, *Electron. Lett.* **12**, 650–651 (1976).
2. T.I. Browning and M.F. Lewis, *Proceedings of the 31st Annual Symposium on Frequency Control*, (Washington, D.C.: Electronic Industries Assoc., 1977), 258–265.
3. K.H. Yen, K.F. Lau, and R.S. Kagiwada, *1979 IEEE Ultrasonics Symposium Proc.*, 778–785.
4. K.F. Lau, K.H. Yen, R.S. Kagiwada, and A.M. Kong, *1980 IEEE Ultrasonics Symposium Proc.*, 240–244.
5. Y. Ebata, K. Sato, and S. Morishita, *1981 IEEE Ultrasonics Symposium Proc.*, 111–116.
6. S. Datta and B.J. Hunsinger, *J. Appl. Phys.* **50**, 5561–5665 (1979).
7. N.E. Glass and A.A. Maradudin, *Electron. Lett.* **17**, 773–774 (1981).
8. J.Z. Wilcox, K.Y. Yen, T.J. Wilcox, and G. Evans, *J. Appl. Phys.* **53**, 2862–2865 (1982).
9. A. Renard, J. Henaff, and B.A. Auld, *1981 IEEE Ultrasonics Symposium Proc.*, 123–128.
10. R.C.M. Li, J.A. Alusow, and R.C. Williamson, *1975 IEEE Ultrasonics Symposium Proc.*, 285–298.
11. B.A. Auld, A. Renard, and J. Henaff, *Electron. Lett.* **18**, 183–184 (1982).
12. G. Cambon, J.M. Saurel, J. Lassale, J. Attal and W. Shahab, *1981 Ultrasonics Symposium Proc.*, 364–367.
13. R.T. Smith and J.S. Welsh, *J. Appl. Phys.* **42**, 2219–2230 (1971).
14. R. Bechmann, A.D. Ballato, T.J. Lukaszek, *Proc. IRE.* **50**, 1812–1822 (1962).
15. M. Lewis, *1977 IEEE Ultrasonics Symposium Proc.*, 744–752.
16. K. Nakamura, M. Kazumi, and H. Shimizu, *1977 IEEE Ultrasonics Symposium Proc.*, 819–822.
17. D. Chang, Y.A. Shui, and W.H. Jiang, *1982 IEEE Ultrasonics Symposium Proc.*, 53–56.
18. B.A. Auld, *Acoustic Fields and Waves in Solids*, (Wiley Interscience, New York, 1973), Vol. 2, p. 297.

# *MISSION*
# *of*
# *Rome Air Development Center*

*RADC plans and executes research, development, test and selected acquisition programs in support of Command, Control Communications and Intelligence ($C^3I$) activities. Technical and engineering support within areas of technical competence is provided to ESD Program Offices (POs) and other ESD elements. The principal technical mission areas are communications, electromagnetic guidance and control, surveillance of ground and aerospace objects, intelligence data collection and handling, information system technology, ionospheric propagation, solid state sciences, microwave physics and electronic reliability, maintainability and compatibility.*

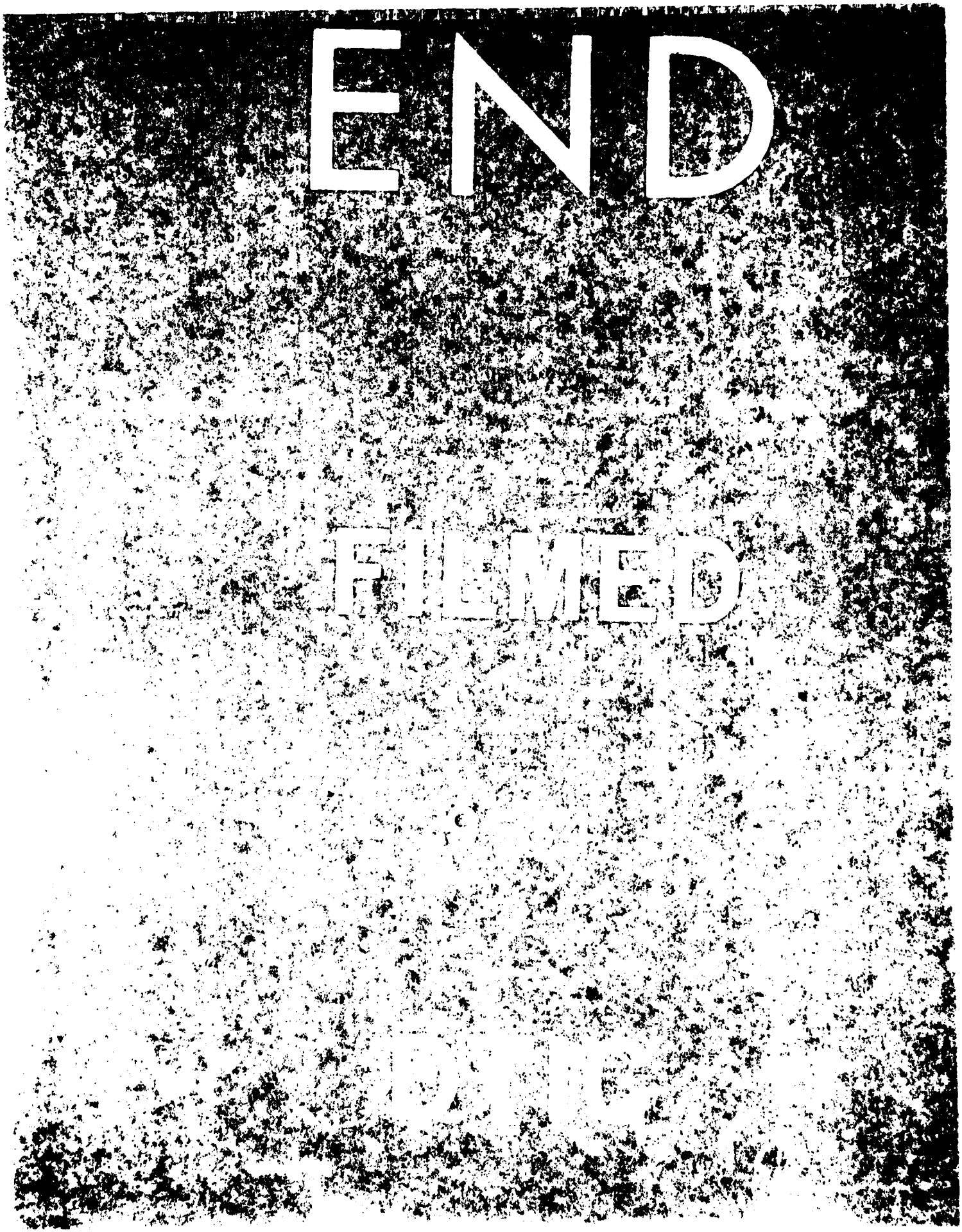
END
FILMED